Microsystem Technologies (2021) 27:3171–3181
https://doi.org/10.1007/s00542-020-05130-y

TECHNICAL PAPER

Single-axis low acceleration sensing using an enhanced piezoelectric vibration energy harvester

Bapi Debnath[1] · R. Kumar[1]

Received: 3 October 2020 / Accepted: 17 November 2020 / Published online: 4 January 2021

Abstract
In this paper, a microscale device comprising a Flared-Ψ shaped composite cantilever having polyvinylidene fluoride (PVDF) ferroelectric polymer thin-film-based unimorph structure and a single brass ring mass is designed and validated by means of finite element method (FEM) simulations and experimental examinations to scavenge energy with high normalized areal and volumetric energy density of 6.8892×10^{-4} (μW/(mm^2 g^2 Hz)) and 6.3021×10^{-4} (μW/(mm^3 g^2 - Hz)), respectively from ambient vibrations. Investigation shows that the proposed device also can be used as a single-axis low-g accelerometer with high sensitivity and good linearity for acceleration sensing applications. The maximum power and voltage output of the device are 2.401 nW and 53.67 mV, respectively over 14.1 Hz resonant frequency at 1.2 MΩ load and 0.05 g input acceleration. The lowest sensible signal and unamplified sensitivity of accelerometer are obtained to be 0.01 g and 60.5035 mV/g, respectively over 13 Hz to subhertz frequency range. The linearity of the sensitivity as a function of acceleration is obtained to be 0.0022% in the full scale.

1 Introduction

An accelerometer entailing high sensitivity can be considered as a vibration sensor. Vibration and acceleration sensors are used for machinery failure prediction, geophysical sensing and MEMS based accelerometers are vastly suitable for biomedical instrumentation, inertial navigation and rollover control of automobile because of their low power-utilization and small size. Various mechanism of accelerometers has been exploited by researchers based on different sensing methods. Chae et al. (2005) introduced three-axis accelerometer employing silicon capacitive system and having micro-g resolution. Chen et al. (1997) investigated over range capacity of an accelerometer functioning on piezoresistive working principle. Satchell and Greenwood (1989) introduced single crystal silicon-based accelerometer employing a mechanical resonator (operated by thermal expansion method) for sensing. Kubena et al. (1996) reported an accelerometer comprising electrostatic electrode-based silicon cantilever beam and which is constructed with a tunneling tip beneath of the cantilever. Zou et al. (2008) reported three-axis and single-axis accelerometers having bimorph based piezoelectric mechanism. Li et al. (2001) analyzed performance of the triaxis accelerometers employing finite-element-method simulations. Among these mechanisms, piezoelectric based accelerometer has the advantages of very high sensitivity, simple detection circuitry and self-generating (which means no requisition of external power) based characteristics. Apart from high-frequency based accelerometers, the low-frequency based accelerometers are also have been wildly investigated by the researchers, because peak frequency range of different vibration sources such as mechanical devices, human activities, and transportation etc. are in very low ranges (1–10 Hz) (Li et al. 2018), where an accelerometer can be used in the condition monitoring system. Preeti et al. (2019) proposed a low frequency-based accelerometer utilized for human health monitoring. Li et al. (2019) proposed a leaf spring based low frequency accelerometer comprising 1–10 Hz of working frequency range. Tian et al. (2016) proposed a high sensitivity based piezoelectric accelerometer, to detect the fault in electrical cable, which causes very weak vibration signal comprising low frequency due to electric

✉ Bapi Debnath
bapi.dn@gmail.com

R. Kumar
rajagopal.kumar@nitnagaland.ac.in

[1] Department of Electronics and Instrumentation Engineering, National Institute of Technology Nagaland, Dimapur, Nagaland 797103, India

spark in it. Wang et al. (2018) proposed a ZnO-nanowires coated cellulose paper based piezoelectric accelerometer having 84.75 Hz natural frequency. These facts inspired us to design a new accelerometer having high sensitivity and good linearity for weak vibration signal detection.

Recent development boost in miniaturization technology of less power consumable systems has been driving more and more research work in the ambient energy harvesting field. By using the ambient energy harvesting devices, the process of either recharging or replacing the conventional batteries could be avoided due to their limited lifecycle (Elfrink et al. 2010). Among different kind of ambient energy harvesting devices like piezoelectric, electrostatic and electromagnetic transduction mechanism-based systems (Mitcheson et al. 2008), the piezoelectric vibration energy harvester (PVEH) have attracted a great research attention due to its uncomplicated structure property with high power generating efficiency and widely available vibration source (Hirasawa et al. 2010; Hajati and Kim 2011; Kanno et al. 2012; Minh et al. 2013; Dow et al. 2014; Wang and Du 2015; Song et al. 2017; Tao et al. 2019). But maximum peak frequency and acceleration value of the common vibration sources lies between 10–150 Hz and 0.01–0.5 g, respectively (Roundy et al. 2003; Kim et al. 2012). Accordingly, PVEHs supposed to be functional in low frequency and acceleration range of the ambient vibration sources, but working frequency and acceleration range of the most reported PVEHs are generally above 150 Hz frequency or else above 1 g acceleration (Marzencki et al. 2008; Lee et al. 2009; Muralt et al. 2009). These facts serve as the motivation for this study of PVEH which can work in low frequency and acceleration based conditions.

In this article, an enhanced PVEH design comprising a Flared-Ψ shaped cantilever supported by an end ring mass is proposed with low volume and weight. We also compared the outcomes of a Flared-Ψ shaped PVEH without ring mass with the same active volume and area based most popular Rectangular-shaped PVEH having no ring mass. Furthermore, a prototype of the proposed Flared-Ψ shaped cantilever based device is fabricated and demonstrated to exhibit 14.1 Hz resonant frequency while maintaining 108.08 mm^3 active volume. Additionally, demonstrated applications of this proposed device are low-frequency-vibration energy scavenging and single-axis low acceleration sensing. The corresponding device design, the vibration mode shape and stress distribution of the PVEH were done in finite element method (FEM) simulator COMSOL Multiphysics. Obtained voltage and power output from the device were validated by means of simulations and experimental examinations. Survey indicates that most PVEH employed piezoelectric material is PZT (Lead Zirconate Titanate) but polyvinylidene fluoride (PVDF) is considered for the proposed Flared-Ψ shaped cantilever based PVEH, because compare to PZT this ferroelectric polymer has 2.6 times larger tensile strength, it can withstand large strain, it is less fragile and it is enviro-friendly material also (Rashmi et al. 2019).

1.1 Structure design

The resonant frequency of a PVEH is an important design parameter because the device should function in resonance with the ambient frequency to reach maximum output or else the potential will noticeably drop off (Priya and Inman 2009). For the first bending mode of a cantilever beam comprising proof mass, the natural frequency (ω_n) can be inscribed as (Priya and Inman 2009):

$$\omega_n = \sqrt{\frac{k_{eq}}{m_{eq}}} = \sqrt{\frac{3EI/L^3}{(33/140)M_bL + M_m}} \tag{1}$$

where. k_{eq} and m_{eq} are spring constant and effective mass of the structure, respectively. EI is the beam flexural rigidity, L is the beam length, M_b represents the mass per unit length, and M_m is the tip mass.

The power output produced by the deformation of piezoelectric structure is subjected to the effective electrode area of piezoelectric materials. For a unimorph cantilever comprising piezoelectric material, the produced output power can be determined from the expression (Kim et al. 2012):

$$P_{output} = f \cdot S^2 \cdot V_p \cdot E_p \cdot k_{xy}^2 \tag{2}$$

and

$$k_{xy}^2 = \frac{Stored\ energy}{Input\ mechanical\ energy} = \frac{E_p d_{xy}^2}{\varepsilon} \tag{3}$$

where f is excitation frequency (Hz), Sisstrain, V_p is volume of the piezoelectric material, E_p is Young's modulus, ε is dielectric permittivity, d_{xy} is piezoelectric constant and k_{xy} is electromechanical coupling coefficient by means of x-poling and y-applied stress direction. Traditionally, there are two different arrangements of piezoelectric modes for MEMS based PVEH such as d_{31} mode (capacitor-design) (Roundy and Wright 2004) and d_{33} mode (interdigitated-design) (Naruse et al. 2009). However, in case of d_{31} mode two electrodes (bottom and top) are mounted on a piezoelectric layer but in case of d_{33} mode interdigitated-styled electrodes are applied. Although utilization of d_{33} mode in PVEH devices can accumulate more electric charge, d_{31} mode have fabrication friendly electrode configuration intended for small sized MEMS based devices. Also, piezoelectric d_{31} mode have a significant functional advantage over d_{33} mode because of its nonresistant characteristics, more strains can be acquiesced with a

smaller amount of employed force. Thus, the resonant frequency is comparatively lower in piezoelectric d_{31} mode. We utilized the d_{31} mode for charge collection from the piezoelectric material (PVDF) layer of proposed PVEH design.

Equation (1) indicates that, in order to lessen the PVEH natural frequency to lower resonant frequency the cantilever based spring beam needs to be designed in such way that it has smaller length dimension along other directions but higher length in effective. Therefore, a bulk brass ring mass comprising area of 14.948 mm^2 and thickness of 6 mm was employed to accomplish moderately a large mass value and a Flared-Ψ shaped cantilever based spring beam was designed to decrease the spring stiffness. In order to compare the outcomes with the widely used Rectangular-shaped PVEH, we also constructed a Flared-Ψ shaped and Rectangular-shaped PVEH devices without ring mass having the same active area (62 mm^2) and volume (11.532 mm^3). Figure 1a demonstrates a 3D (3-dimensional) structure of the proposed Flared-Ψ shaped PVEH including all layers of the cantilever. And all detailed device dimensions such as dimensions of the Flared-Ψ shaped proposed device, Flared-Ψ shaped and Rectangular-shaped PVEHs without ring mass are shown in Fig. 1b–d, respectively and tabularized in Table 1. An Indian patent application was filed for a previous version of this structure (comprises a straight clamping end to the base) showing the concept of a Ψ-shaped cantilever based PVEH to achieve a low resonant frequency (below 200 Hz) (Kumar and Debnath 2018). The proposed Flared-Ψ shaped cantilever comprises a flared clamping end to the base and it helps the PVEH device to utilize most of the up-down displacement induced stress at the base-clamp end. As depicted in Fig. 1, two silver (9 μm) electrodes (i.e. upper and lower) are patterned into a capacitor style (i.e. PVDF thin film is placed between two electrodes) on top of a single Flared-Ψ shaped spring comprising mylar polyester (125 μm) layer in order to generate strain in perpendicular to the electric field of PVDF film (28 μm), which forms the d_{31} mode of the piezoelectric element. An acrylic protection layer (15 μm) is used on the top of the upper silver (Ag) electrode. Two electrodes are connected to their respective solder tabs to accumulate the d_{31} mode generated charge. Consequently, when ambient vibration is employed to the PVEH device, certain portions (i.e. free end of the Flared-Ψ shaped cantilever connected to a mass) will move moderately to the base frame and this movement cause deformation or compression in the piezoelectric material. This particular circumstance give rise to the piezoelectric effect which generates electrical potential.

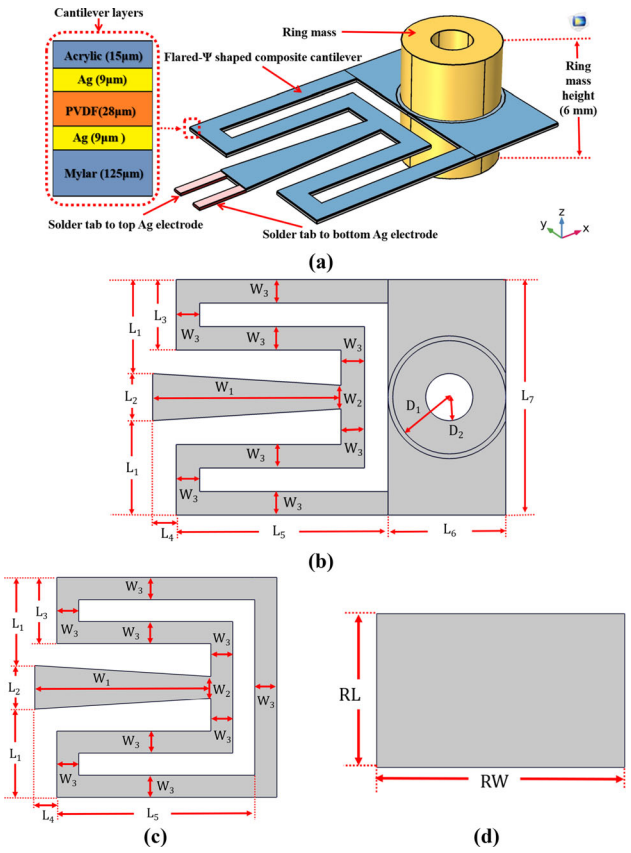

Fig. 1 **a** Schematic 3D-design of the proposed Flared-Ψ shaped PVEH device comprising all the cantilever layers viz., acrylic/Ag / PVDF/Ag/mylar, geometrical dimension details of the (**b**) proposed Flared-Ψ shaped device, **c** Flared-Ψ shaped PVEH without ring mass, and **d** rectangular-shaped PVEH without ring mass

The electric charge produced from the PVEH can be used as a vibration sensor or else a single axis accelerometer. In order to optimize the mechanical design and predict the device performance, we analyze the sensitivity and mechanical resonant frequency for the single axis piezoelectric accelerometer (i.e. proposed PVEH). To characterize the accelerometer measurement range in terms of acceleration, accelerometer sensitivity is considered as what rate mechanical energy is transformed into electric energy. Accelerometer sensitivity is generally stated as millivolts per acceleration because of gravity (mV/g) or picocoulombs per acceleration caused by gravity (pC/g), where g denotes 9.81 m/s^2. The transfer function (input/output relationship) of the accelerometer is not absolutely linear. It is well-known that linearity error can be interpreted in terms of percentage of nonlinearity. And it is defined as the ratio of maximum deviation of output (D_m) response from a best fit straight line to full scale output (FSO) of the device. It is expressed in a percentage of FSO and the equation can be stated as:

$$Nonlinearity(\%) = \frac{D_m}{FSO} \times 100 \tag{4}$$

Table 1 Dimension details of the PVEH devices

Geometrical parameters	Values (mm)	Geometrical parameters	Values (mm)
L_1	4	W_1	8
L_2	2	W_2	1
L_3	3	W_3	1
L_4	1	D_1	2.4
L_5	9	D_2	1
L_6	5	RL	6.2
L_7	10	RW	10

2 Simulation and fabrication

2.1 Finite Element Method (FEM) simulation

Before going for fabrication, the design of the Flared-Ψ shaped PVEH device is modeled and simulated in COMSOL Multiphysics 5.4 (commercial version) using 3D Space Dimension to evaluate its performance. The model of Flared-Ψ shaped cantilever based PVEH device, Flared-Ψ device without ring mass and Rectangular-shaped device without ring mass are constructed in COMSOL using the layer and dimension properties available in Fig. 1 and Table 1. Material properties (like piezoelectric coefficients, dielectric permittivities, 2–4 10^9 N/m^2 Young's modulus and 1.78 10^3 kg/m mass density of PVDF etc.) used for PVDF are based on the data available in the data sheet of LDTM-028 K and LDT0-028 K/L (Sparkfun.com 1999, 2008). Utilizing COMSOL, Multiphysics of Piezoelectric Devices (pze1) and Electrical Circuit (cir) are employed to ascertain responses (mechanical and electrical) of the PVEH device. Moreover, physics of Piezoelectric Devices (pze1) is assemblage of two other physics such as Solid Mechanics (solid) and Electrostatics (es). Fixed Constraint Boundary condition is used in the physics of Solid Mechanics (solid), to fixed the surfaces of the supporting frame while remaining surfaces are set free for the movement. In the physics of Solid Mechanics (solid), Body Load of the proposed PVEH device can be applied in terms of device weight due to gravity (i.e. gravity-induced structure pre-bending condition) and a sinusoidal vertical acceleration to generate strain in the piezoelectric (PVDF) layers. The piezoelectric d_{31} mode of PVDF is achieved using the Terminal and Ground Boundary condition at top and bottom horizontal face of upper and lower PVDF layers, respectively in the physics of Electrostatics (es). In the physics of Electrical Circuit (cir), a Resistor is included linking the Ground Node and External I-Terminal through Terminal voltage (es/term1), to define the resistor value across which electrical responses can be observed. The

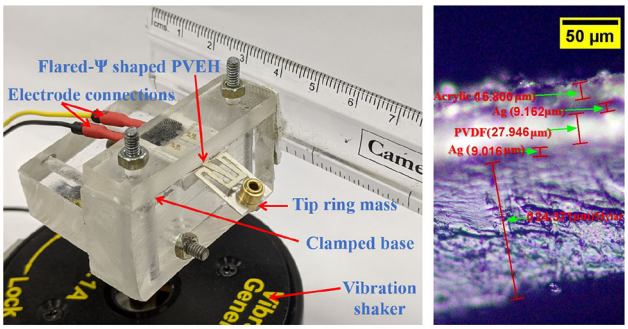

Fig. 2 **a** Close-up picture of the Flared-Ψ shaped PVEH, **b** microscopic layout image of the Flared-Ψ shaped cantilever

User-controlled size of the Mesh elements is reduced until the model is giving almost a saturated result. Free Triangular and Free Tetrahedral blocks with extremely fine element size are used for finite element meshing. Parametric study of Stationery, Eigenfrequency and Frequency Domain analysis in COMSOL are performed to obtain the total deformation over external stress, natural frequency and electrical responses of the device, respectively. Finally, utilizing COMSOL the total number of DOF (degrees of freedom) solved for proposed Flared-Ψ shaped PVEH device, Flared-Ψ device without ring mass and Rectangular-shaped device without ring mass are obtained to be 149,484, 250,560, 92,412, respectively.

2.2 Prototype fabrication

As depicted in Fig. 2a, a proof-of-concept PVEH has been fabricated by assembling a commercial cantilever-type PVDF piezoelectric sensor beam LDTM-028 K (Sensor Solutions—TE Connectivity) with ∼ 125 µm polyester housing and a cylindrical ring mass (entailing 0.72 g) connected at the tip end of the beam. The used brass ring mass has the height of 6 mm, diameter of ∼ 2.4 mm and a hole of ∼ 1 mm inner radius. The proposed Flared-Ψ shaped PVEH structure has been developed from the LDTM-028 K beam by utilizing precision cutting process

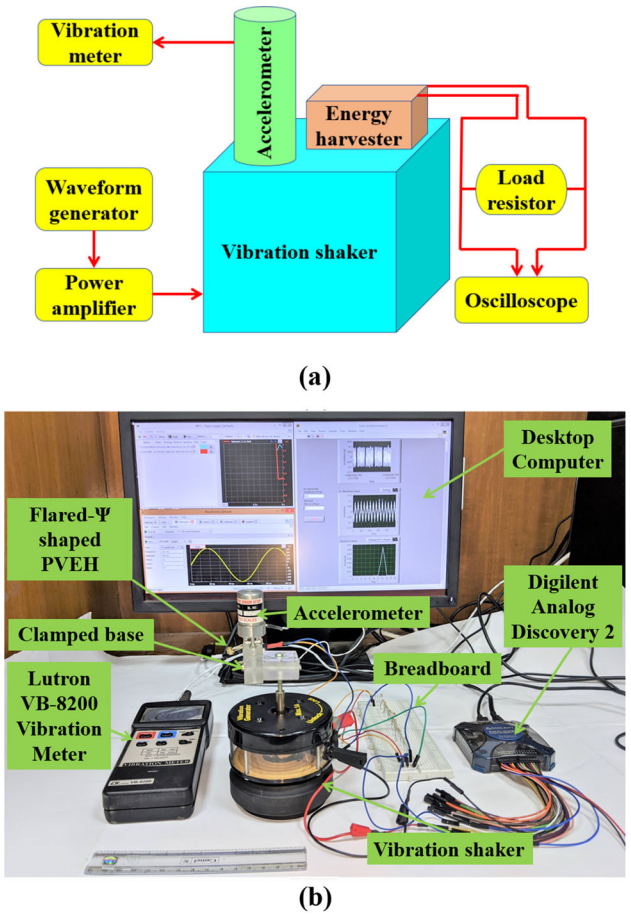

Fig. 3 **a** Schematic model and **b** photograph of the experimental platform used to analyze the performances of the proposed Flared-Ψ shaped PVEH device

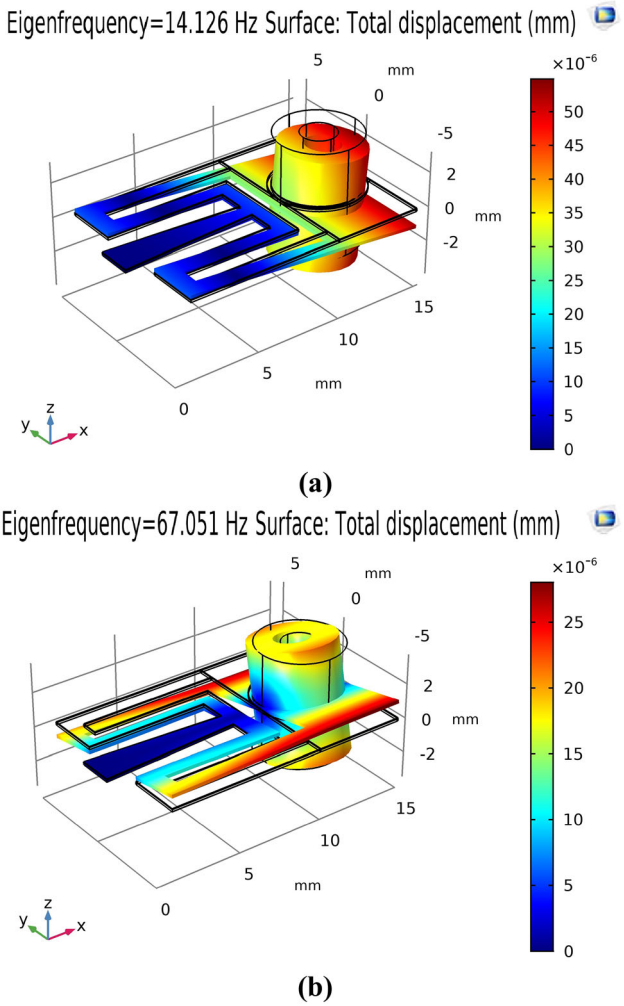

Fig. 4 COMSOL simulated total displacement over **a** first and **b** second vibration mode shape of the Flared-Ψ shaped device

and tools. The employed PVDF in the LDTM-028 K beam has ∼ 28 μm thickness and its top and bottom surfaces are covered by silver-ink electrodes. To collect the stress induced potential from the PVDF, the top and bottom silver-ink electrodes are connected to their respective contact pads. The electrodes are electrically isolated by protective layer of acrylic film. The microscopic image of the cross section of the used PVDF film-based beam is shown in the Fig. 2b.

3 Experimental setup and procedure

For performance evaluation of the proposed Flared-Ψ shaped PVEH at various accelerations and input frequencies, the output from the fabricated prototype has been acquired and analyzed while the PVEH was vibrated with a shaker. The Fig. 3a and b shows the schematic model and photograph of experimental platform used for the PVEH characterization, respectively. The shaker was excited at the level of required magnitude and frequency by applying an inbuilt sinusoidal waveform generator in Digilent Analog Discovery 2. An accelerometer connected to vibration Meter (Lutron VB-8200) was employed to spindle of the shaker to monitor the acceleration. A Desktop Computer consisting WaveForms software connected to Digilent Analog Discovery 2 is utilized as oscilloscope to measure the outputs from the proposed Flared-Ψ shaped PVEH while vibrating. As illustrated in The Fig. 3b, the output power and voltage over external load resistance were measured across the resistor arranged in breadboard.

4 Results and discussion

This study aims to design a miniature PVEH for low acceleration and frequency based vibration ambiences. Accordingly, the proposed Flared-Ψ shaped cantilever based PVEH device was characterized by simulations and experimentations. Subsequently, it is also observed that

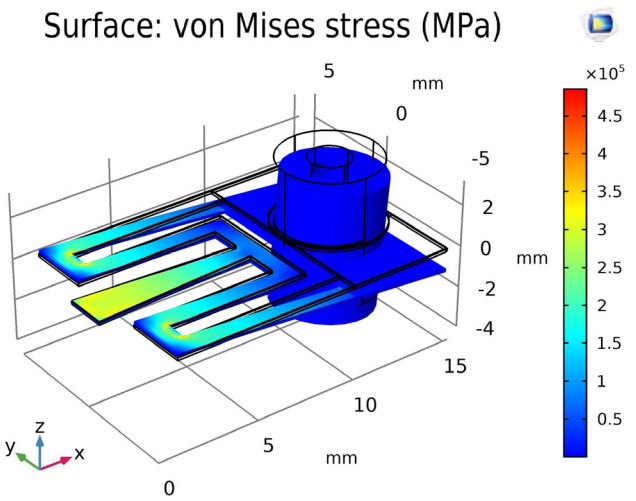

Fig. 5 COMSOL simulated stress distribution in 3D-view of the Flared-Ψ shaped device at 1 MPa boundary load

apart from delivering power to the power-hungry devices, the proposed device can be used to provide direct information about acceleration. Correspondingly, the sensitivity and linearity test regarding acceleration output were performed.

4.1 Simulation and experimental evaluation

To examine the 1st and 2nd natural frequency of the Flared-Ψ shaped device FEM simulator COMSOL is utilized and the simulation shows 1st natural frequency of 14.126 Hz and 2nd natural frequency of 67.051 Hz for the proposed device. Figure 4a and b depicts COMSOL simulated 1st and 2nd vibration mode shape of the device-body, respectively. The 2nd mode shows a torsional movement of brass ring mass but in 1st mode, up-down movement of brass ring mass is observed. Also, it is observed that in 1st mode the ring mass cover maximum displacement, consequently it will contribute to harvest more electrical response compare to 2nd mode. Therefore, we choose natural frequency of 1st mode (i.e. 14.1 Hz) for rest of the evaluation. To examine the cantilever entailed stress concentration, 1 MPa boundary load is applied on top surface of the PVEH utilizing COMSOL and a fair stress distribution over Flared-Ψ shaped composite cantilever is observed, as depicted in Fig. 5.

We have investigated the electrical responses of the proposed device, utilizing both the COMSOL based 3D model and fabricated prototype (which was coupled to an experimental setup). Figure 6 demonstrates the Flared-Ψ shaped PVEH generated rms voltage (V_{rms}) output employing 13–15 Hz frequency at a constant 1 MΩ load resistance and 0.05 g acceleration. The simulated and measured results show maximum 50.37 mV (simulated)

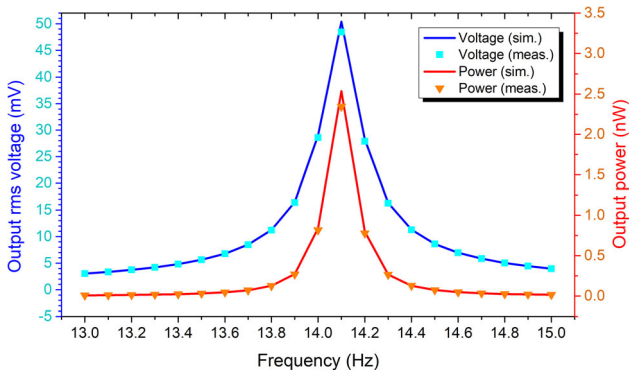

Fig. 6 Simulated (sim.) and measured (meas.) rms voltage and power output from the Flared-Ψ shaped device as a function of frequency at constant input acceleration of 0.05 g and load resistance of 1 MΩ

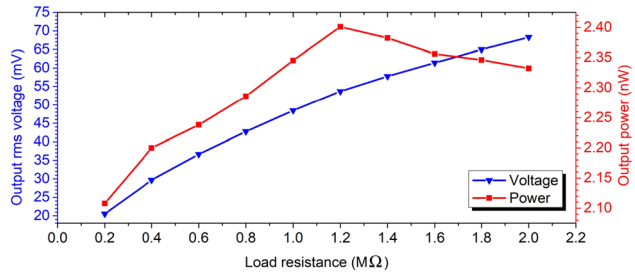

Fig. 7 Experimental results of the output rms voltage and power with the variation of load resistance at fixed 14.1 Hz resonant frequency and 0.05 g acceleration for Flared-Ψ shaped device

and 48.42 mV (measured) rms voltage output, and 2.537 nW (simulated) and 2.345 nW (measured) power output at its 14.1 Hz resonant frequency while having a relatively low input acceleration of 0.05 g. To determine the optimum load resistance, device power output (V_{rms}^2/R) across various load resistance (R) were analyzed. Figure 7 demonstrates the results of the rms voltage and power responses with the variation of load resistance at constant 14.1 Hz resonant frequency and 0.05 g input acceleration. The results show maximum power output of 2.401 nW and voltage output of 53.67 mV at 1.2 MΩ optimum load resistance.

It is observed that at as low as 0.05 g input acceleration, the produced power from the proposed harvester was enough to fulfill the energy consumption requirement of various low power micro devices. Apart from power scavenging applications, to demonstrate that the proposed device can be used for low frequency based vibration and acceleration sensing applications, we also investigated the rms voltage output of the device across 0–25 Hz frequencies, taken in 0.5 Hz increments at constant 1 g acceleration and 1 MΩ load resistance while maintaining the ring mass up-down movement towards Z-direction i.e. gravitational direction. Figure 8 shows the rms voltage and power

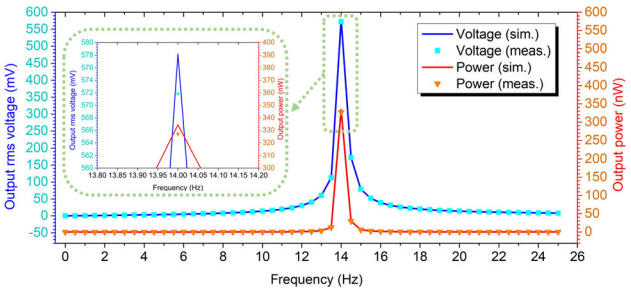

Fig. 8 Simulated (sim.) and measured (meas.) results of rms voltage and power output with the variation of frequency response at 1 g constant acceleration and 1 MΩ load resistance

output with variation of frequencies. The simulated and measured results demonstrate a peak of 578.18 mV (simulated) and 571.83 mV (measured) rms voltage output, 334.29 nW (simulated) and 326.99 nW (measured) power output at 14 Hz resonant frequency, and a steep response from subhertz to 13 Hz. In order to explore the accurate and reliable results of the accelerometer device, the working frequency should be lower than the resonant frequency (Tian et al. 2016). Therefore, based on above investigated results we choose 13 Hz (one of the steep frequency response) to explore the device output with variation of low acceleration. Figure 9 shows the rms voltage and power output with variation of 0.01–0.1 g acceleration over constant 13 Hz frequency and 1 MΩ load resistance. From these results it can be observed that a minimum voltage of 0.6 mV was generated at 0.01 g while a maximum voltage of 6 mV was generated at 0.1 g. Moreover, Figs. 8 and 9 demonstrates that with utilization of proper current or voltage detection circuitry the minimum detectable acceleration and frequency of our proposed device are 0.01 g and 0.1 Hz, respectively. In order to accomplish low frequency vibration sensing, the unamplified sensitivity of 60.5035 mV/g from Flared-Ψ shaped cantilever based PVEH was obtained by applying acceleration from 1 to 5 g (as illustrated in Fig. 10) at constant frequency of 13 Hz and load resistance of 1 MΩ.

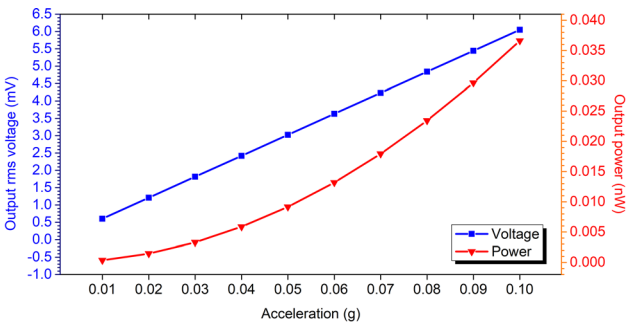

Fig. 9 Experimental voltage and power output of the Flared-Ψ shaped device versus low acceleration amplitude over constant frequency of 13 Hz with a 1 MΩ load resistance

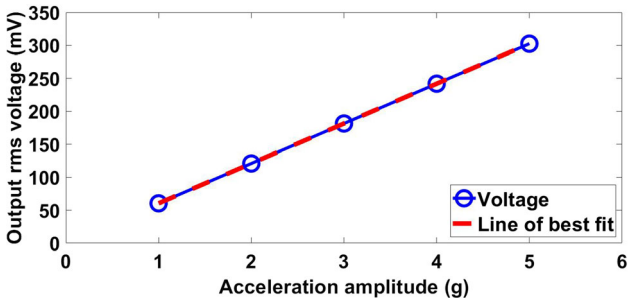

Fig. 10 Experimental output of the Flared-Ψ shaped device versus acceleration amplitude of 1–5 g over constant frequency of 13 Hz with a 1 MΩ load resistance showing an unamplified sensitivity of 60.5035 mV/g and linearity 0.0022% in the full scale

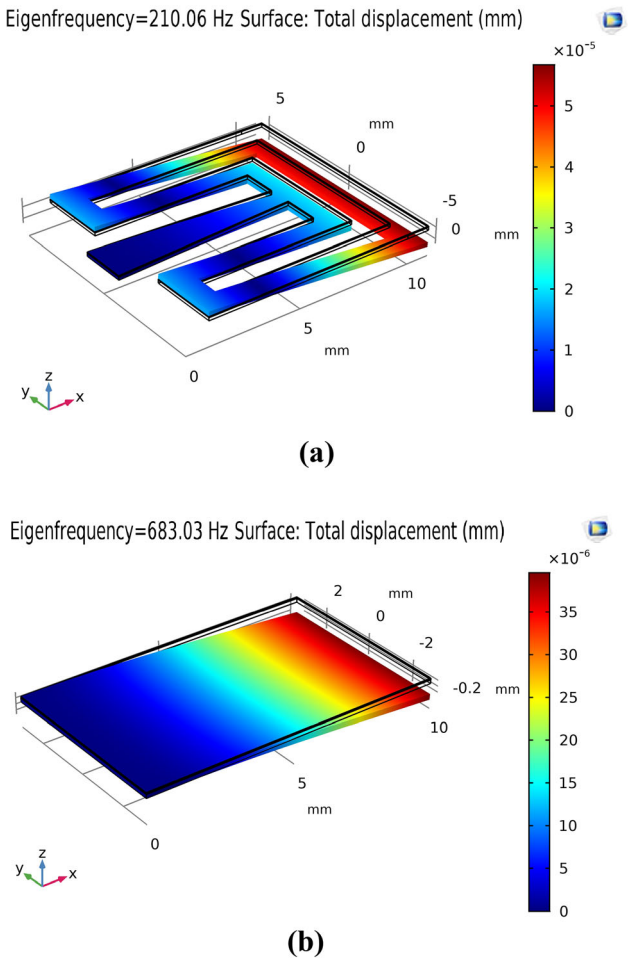

Fig. 11 COMSOL simulated total displacement over first vibration mode shape of the **a** Flared-Ψ shaped PVEH without ring mass, and **b** Rectangular-shaped PVEH without ring mass

We also calculated the linearity of the sensitivity in terms of acceleration. Figure 11 also shows the obtained linearity of the sensitivity (i.e. 0.0022%) in percentage of the full scale up to 5 g input accelerations. From Figs. 6 and 8, it is

Table 2 Comparison of different MEMS vibration energy harvester performance

References	Active area (mm^2)	Active volume (mm^3)	Acceleration (g)	Frequency (Hz)	Load (kΩ)	Voltage (V)	Power (μW)	Normalized areal power density ($\mu W/(mm^2 \cdot g^2 \cdot Hz)$)	Normalized volumetric power density ($\mu W/(mm^3 \cdot g^2 \cdot Hz)$)	Sim/ Meas
Marzencki et al. (2008)	0.96	0.5	2	1495	450	0.853	0.8	1.3935×10^{-4}	2.6755×10^{-4}	Meas
Lee et al. (2009)	4.5	0.43	2.5	256	150	1.79	2.76	3.8333×10^{-4}	4.0116×10^{-3}	Meas
	4.5	0.61	2	214	510	2.29	1.29	3.3489×10^{-4}	2.4705×10^{-3}	
Muralt et al. (2009)	0.96	0.264	2	870	NA	1.6	1.4	4.1906×10^{-4}	1.5238×10^{-3}	Meas
Hirasawa et al. (2010)	NA	1.63	1	857	1100	NA	0.18	NA	1.2885×10^{-4}	Meas
Hajati and Kim (2011)	120	0.02	4	1300	290	0.8	22	8.8141×10^{-6}	5.2884×10^{-2}	Meas
Kanno et al. (2012)	56.1	11.4	1	1036	1.7	NA	1.1	1.8926×10^{-5}	9.3138×10^{-5}	Meas
Minh et al. (2013)	0.81	0.306	1.02	1509	90	0.25	0.731	5.7483×10^{-4}	1.5216×10^{-3}	Meas
Dow et al. (2014)	27.28	12.76	2	572	495	NA	34.78	5.5722×10^{-4}	1.1913×10^{-3}	Meas
Wang and Du (2015)	11.5	11.5	1.02	1300	380	≈1.25	0.98	6.3006×10^{-5}	6.3006×10^{-5}	Meas
	11.5	11.5	1.02	1313.4	600	≈1.75	1.25	7.9545×10^{-5}	7.9545×10^{-5}	
Song et al. (2017)	10.75	0.11	0.25	68	40	NA	0.023	5.0342×10^{-4}	4.9197×10^{-2}	Meas
Tao et al. (2019)	NA	105.125[a]	0.5	490	240	NA	0.00046	NA	3.5720×10^{-8}	Meas
	NA	105.125[a]	0.5	403.8	250	0.010	NA	NA	NA	
	NA	105.125[a]	0.5	489.9	250	0.015	NA	NA	NA	
Flared-Ψ (This work)	98.869	108.08	0.05	14.1	1200	0.0536778	0.002401	6.8892×10^{-4}	6.3021×10^{-4}	Meas
	98.869	108.08	0.05	14.1	1000	0.04842	0.002345	6.7285×10^{-4}	6.1551×10^{-4}	Meas
	98.869	108.08	0.05	14.1	1000	0.05037	0.002537	7.2794×10^{-4}	6.6591×10^{-4}	Sim
Flared-Ψ PVEH without ring mass (This work)	62	11.532	1	210	1000	0.1059	0.005617	4.3141×10^{-7}	2.3194×10^{-6}	Sim
Rectangular PVEH without ring mass (This work)	62	11.532	1	683	1000	0.0889	0.003959	9.3491×10^{-8}	5.0264×10^{-7}	Sim

NA denotes data not available in the literature

[a]Denotes estimated values

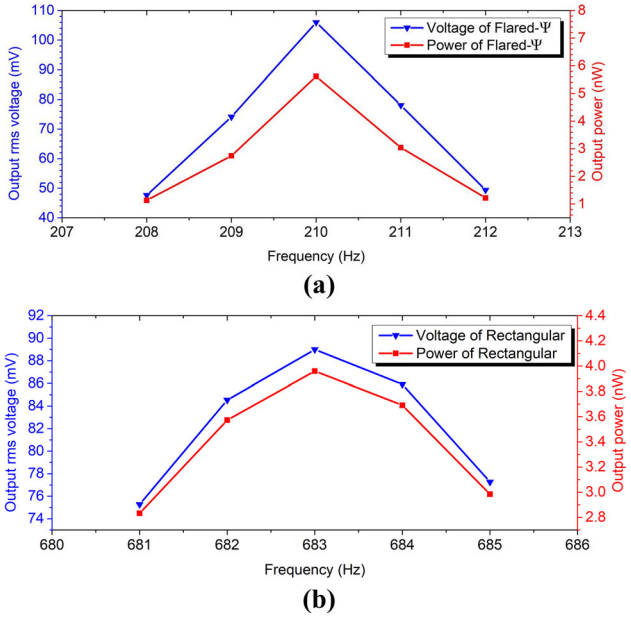

Fig. 12 COMSOL simulated rms voltage and power output with the variation of frequency response at 1 g constant acceleration and 1 MΩ load resistance for the **a** Flared-Ψ shaped PVEH without ring mass, and **b** Rectangular-shaped PVEH without ring mass

also seen that the FEM simulator COMOL simulated outcomes agree well with the experimental outcomes.

4.2 Comparison of the performance

As suggested by Song et al. (2017), we normalized the energy (i.e. power) density to compare the energy output of our proposed work with other previous reported work. The normalized energy density based on active or operative area and volume of the device were obtained to be 6.8892 $\times 10^{-4}$ $(\mu W/(mm^2 \cdot g^2 \cdot Hz))$ and 6.3021 $\times 10^{-4}$ $(\mu W/(mm^3 \cdot g^2 \cdot Hz))$, respectively. The performance comparison of the various PVEH devices are framed in Table 2. It is observed that the proposed Flared-Ψ shaped cantilever based PVEH device has comparatively low resonant frequency, low input acceleration and high normalized areal energy density output. But in some cases, it shows comparatively low volumetric energy density output. However, to compare the PVEH outcomes fairly, there are several other factors which should be same for the devices such as material properties of the used substrate, electrodes, protection layer and piezoelectric material. To demonstrate the competency of the Flared-Ψ shaped cantilever and for a fair comparison, we investigate the 1st natural frequency and electrical outputs of the Flared-Ψ shaped and Rectangular-shaped PVEHs without ring mass having the same material properties. To investigate the natural frequency and electrical response of these devices, COMSOL based simulations were used because Table 2 demonstrates that our simulation technique-based results agree well with the experimental results. As illustrated in Fig. 11, the Flared-Ψ shaped device without ring mass shows a very low 1st natural frequency (i.e. 210.06 Hz) compare to the 683.03 Hz 1st natural frequency of Rectangular-shaped device while comprising the same active area (62 mm^2) and volume (11.532 mm^3). And as illustrated in Fig. 12, the Flared-Ψ shaped device having no ring mass shows maximum 105.9 mV rms voltage and 5.617 nW power compare to the 88.9 mV rms voltage and 3.959 nW power of Rectangular-shaped device at their respective natural frequency while employing 1 g input acceleration and 1 MΩ load resistance. The performance comparison of these two PVEHs are also framed in Table 2, which demonstrates comparatively a very good performance of Flared-Ψ shaped device without ring mass over Rectangular-shaped device. The performance comparison between proposed device and already published piezoelectric accelerometers are shown in Table 3.

Table 3 Comparison of Miniature Piezoelectric accelerometers performances

Reference	Piezoelectric material	Sensitivity (mV/g)	Linearity	Minimum detectable acceleration (g)	Resonant frequency (Hz)	Frequency range
Zou et al. (2008)	ZnO	7.0	0.9 % up to 3g	0.01	98	Subhertz to 60 Hz
Tian et al. (2016)	PZT	8.9271[a]	0.0205 %	NA	1279.1	NA
Wang et al. (2018)	ZnO	16.3	NA	NA	84.75	NA
This work	PVDF	60.5035	0.0022 % up to 5g	0.01	14.1	Subhertz to 13 Hz

NA denotes data not available in the literature

[a]Denotes estimated values

4.3 Usability of the device

The proposed Flared-Ψ shaped device can be used for weak vibration source (such as earthquake, civil structures, railway and ship operation systems etc.) based condition monitoring and energy scavenging applications. As an autonomous-sensor-system demonstrated by Elfrink et al. (2010), the proposed device can be used remotely for accumulating the acceleration information or else it can be used to deliver power to the micro power-hungry devices. Furthermore, like Chae et al. (2005) demonstrated a single chip three-axis accelerometer system comprising three single-axis accelerometers, our proposed vibration energy harvester cum single-axis accelerometer consisting Flared-Ψ shaped composite piezoelectric cantilever also can be used for three-axis acceleration sensing application.

5 Conclusion

An enhanced Flared-Ψ shaped unimorph piezoelectric cantilever based device have been modeled, fabricated and investigated for low frequency and acceleration based applications such as low vibration energy scavenging and low-g acceleration sensing. The proposed device is constructed in such way that it can exploit the low frequencies and accelerations of ambient vibration sources. First the device was designed and analyzed using a FEM software COMSOL and then accordingly fabricated. The outputs of the Flared-Ψ shaped device were characterized by FEM simulations and experimentations. Furthermore, the enviro-friendly piezoelectric material PVDF used in the middle of the two silver electrodes demonstrates 53.67 mV voltage and 2.401 nW maximum power under 1.2 MΩ optimum load resistance, when the Flared-Ψ shaped PVEH device was excited by a base excitation based vibration with 14.1 Hz frequency and 0.05 g acceleration. Moreover, variation of low frequency and acceleration based investigation demonstrates that the proposed PVEH device can be used for low vibration and acceleration sensing with of 60.5035 mV/g sensitivity and 0.0022% linearity in the full scale. Furthermore, a comparative study between two same active area and volume based PVEHs shows a very good performance of Flared-Ψ shaped device without ring mass over well-known Rectangular-shaped device.

References

Chae J, Kulah H, Najafi K (2005) A monolithic three-axis micro-g micromachined silicon capacitive accelerometer. J Microelectromech Syst 14(2):235–242

Chen H, Shen S, Bao M (1997) Over-range capacity of a piezoresistive microaccelerometer. Sens Actuat A 58(3):197–201

Dow ABA, Bittner A, Schmid U, Kherani NP (2014) Design, fabrication and testing of a piezoelectric energy microgenerator. Microsyst Technol 20(4–5):1035–1040

Elfrink R, Renaud M, Kamel TM, Nooijer CD, Jambunathan M, Goedbloed M, Hohlfeld D, Matova S, Pop V, Caballero L, Schaijk RV (2010) Vacuum-packaged piezoelectric vibration energy harvesters: damping contributions and autonomy for a wireless sensor system. J Micromech Microeng 20(10):104001

Hajati A, Kim S-G (2011) Ultra-wide bandwidth piezoelectric energy harvesting. Appl Phys Lett 99(8):083105

Hirasawa TH, Yen YTT, Wright PK, Pisano AP, Lin L (2010) Design and fabrication of piezoelectric aluminum nitride corrugated beam energy harvester. In: Proc. Power MEMS, pp 211–214

Kanno I, Ichida T, Adachi K, Kotera H, Shibata K, Mishima T (2012) Power-generation performance of lead-free (K, Na)NbO_3 piezoelectric thin-film energy harvesters. Sens Actuat A 179:132–136

Kim S-G, Priya S, Kanno I (2012) Piezoelectric MEMS for energy harvesting. MRS Bull 37(11):1039–1050

Kubena R, Atkinson G, Robinson W, Stratton F (1996) A new miniaturized surface micromachined tunneling accelerometer. IEEE Electron Device Lett 17(6):306–308

Kumar R, Debnath B (2018) High efficiency piezoelectric energy harvester having?-Shaped cantilever structure. India. Patent 201831041423

Lee BS, Lin SC, Wu WJ, Wang XY, Chang PZ, Lee CK (2009) Piezoelectric MEMS generators fabricated with an aerosol deposition PZT thin film. J Micromech Microeng 19(6):065014

Li G, Li Z, Jin Y, Hao Y, Zhang D, Wu G (2001) Design and simulation of capacitive, piezoresistive and piezoelectric triaxial accelerometers using a highly symmetrical quad-beam structure. Transducers '01 Eurosensors XV, pp 304–307

Li R, Lei Y, Chang Z, Zhang L, Fan K (2018) Development of a high-sensitivity optical accelerometer for low-frequency vibration measurement. Sensors 18(9):2910

Li R, Chang Z, Lei Y, Cheng Z, Liu X, Fan K, Lv J (2019) A low-frequency micro accelerometer based on three-lobed leaf spring and a focus probe. IEEE Photonics J 11(1):1–12

Marzencki M, Ammar Y, Basrour S (2008) Integrated power harvesting system including a MEMS generator and a power management circuit. Sens Actuat A 145–146:363–370

Minh LV, Hara M, Horikiri F, Shibata K, Mishima T, Kuwano H (2013) Bulk micromachined energy harvesters employing (K, Na)NbO_3 thin film. J Micromech Microeng 23(3):035029

Mitcheson P, Yeatman E, Rao G, Holmes A, Green T (2008) Energy harvesting from human and machine motion for wireless electronic devices. Proc IEEE 96(9):1457–1486

Muralt P, Marzencki M, Belgacem B, Calame F, Basrour S (2009) Vibration energy harvesting with PZT micro device. Procedia Chem 1(1):1191–1194

Naruse Y, Matsubara N, Mabuchi K, Izumi M, Suzuki S (2009) Electrostatic micro power generation from low-frequency vibration such as human motion. J Micromech Microeng 19(9):094002

Preeti M, Guha K, Baishnab K, Dusarlapudi K, Narasimha Raju K (2019) Low frequency MEMS accelerometers in health monitoring—a review based on material and design aspects. Mater Today 18:2152–2157

Priya S, Inman DJ (2009) Energy harvesting technologies. Springer, New York

Rashmi K, Rao A, Jayarama A, Pinto R (2019) Piezoelectric P(VDF-TrFE) micro cantilevers and beams for low frequency vibration sensors and energy harvesters. Sens Actuat A 295:574–585

Roundy S, Wright PK, Rabaey J (2003) A study of low level vibrations as a power source for wireless sensor nodes. Comput Commun 26(11):1131–1144

Roundy S, Wright PK (2004) A piezoelectric vibration based generator for wireless electronics. Smart Mater Struct 13(5):1131–1142

Satchell D, Greenwood J (1989) A thermally-excited silicon accelerometer. Sens Actuat 17(1–2):241–245

Song H-C, Kumar P, Maurya D, Kang M-G, Reynolds WT, Jeong D-Y, Kang C-Y, Priya S (2017) Ultra-low resonant piezoelectric MEMS energy harvester with high power density. J Microelectromech Syst 26(6):1226–1234

Sparkfun.com (1999) Piezo film sensors technical manual. 0-1002794-1 datasheet. Available: https://www.sparkfun.com/datasheets/Sensors/Flex/MSI-techman.pdf. **[Accessed: 13 Apr 2020]**

Sparkfun.com (2008) LDT with crimps vibration sensor/switch. 1005447-1 datasheet. Available: https://cdn.sparkfun.com/datasheets/Sensors/ForceFlex/LDT_Series.pdf. **[Accessed: 13 Apr 2020]**

Tao K, Yi H, Tang L, Wu J, Wang P, Wang N, Hu L, Fu Y, Miao J, Chang H (2019) Piezoelectric ZnO thin films for 2DOF MEMS vibrational energy harvesting. Surf Coat Technol 359:289–295

Tian B, Liu H, Yang N, Zhao Y, Jiang Z (2016) Design of a piezoelectric accelerometer with high sensitivity and low transverse effect. Sensors 16(10):1587

Wang P, Du H (2015) ZnO thin film piezoelectric MEMS vibration energy harvesters with two piezoelectric elements for higher output performance. Rev Sci Instrum 86(7):075002

Wang Y, Song P, Li X, Ru C, Ferrari G, Balasubramanian P, Amabili M, Sun Y, Liu X (2018) A paper-based piezoelectric accelerometer. Micromachines 9(1):19

Zou Q, Tan W, Kim ES, Loeb G (2008) Single- and triaxis piezoelectric-bimorph accelerometers. J Microelectromech Syst 17(1):45–57